Science Advances
AAAS

# Supplementary Materials for

## The ABC transporter MsbA adopts the wide inward-open conformation in *E.* coli cells

Laura Galazzo *et al.*

Corresponding author: Enrica Bordignon, enrica.bordignon@unige.ch; Markus A. Seeger, m.seeger@imm.uzh.ch

*Sci. Adv.* **8**, eabn6845 (2022)
DOI: 10.1126/sciadv.abn6845

**The PDF file includes:**



**Other Supplementary Material for this manuscript includes the following:**

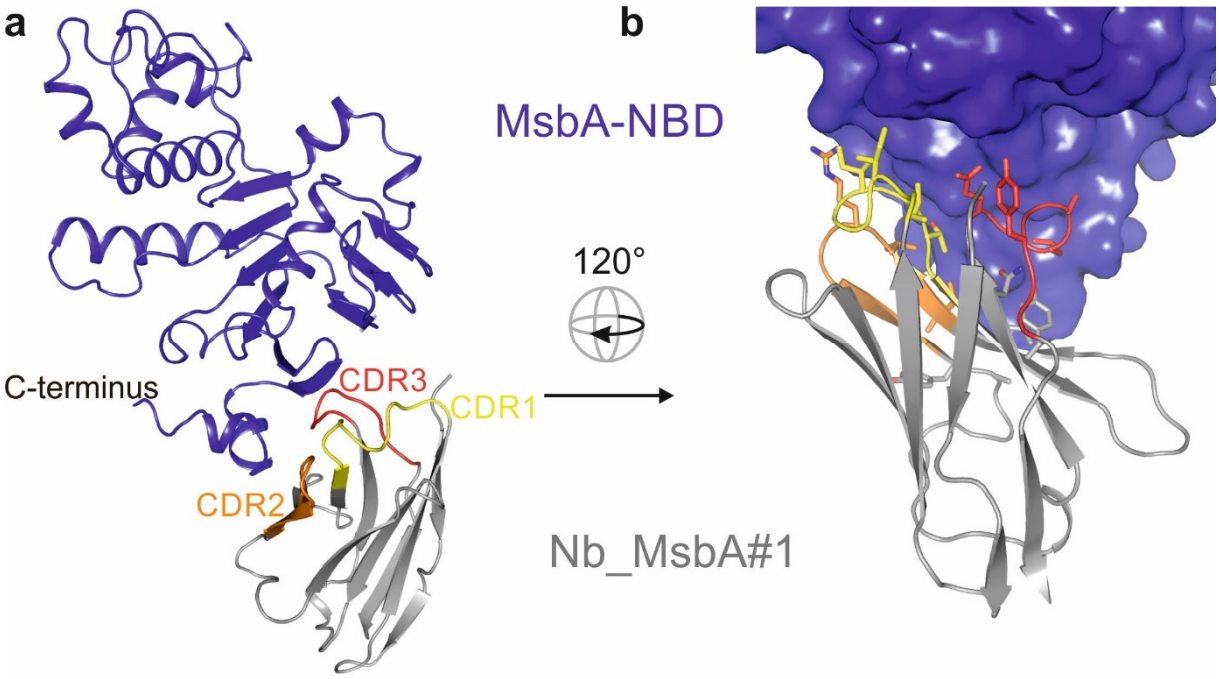


**Figure S1 | X-ray structure of nanobody-NBD complex**. **a,** Cartoon representation of NBD of MsbA (blue) and the nanobody Nb_MsbA#1 (grey). CDR 1, 2 and 3 of the nanobody are yellow, orange and red, respectively. **b,** Close-up view on the interaction interface with nanobody residues establishing intermolecular contacts depicted as sticks. According to the PDBePISA server (https://www.ebi.ac.uk/pdbe/pisa/), the interface area measures 742 Å$^2$ and intermolecular contacts are established by 14 hydrogen bonds and 6 salt bridges (analysis of the interface between chain B and chain C of the asymmetric unit).

**a**

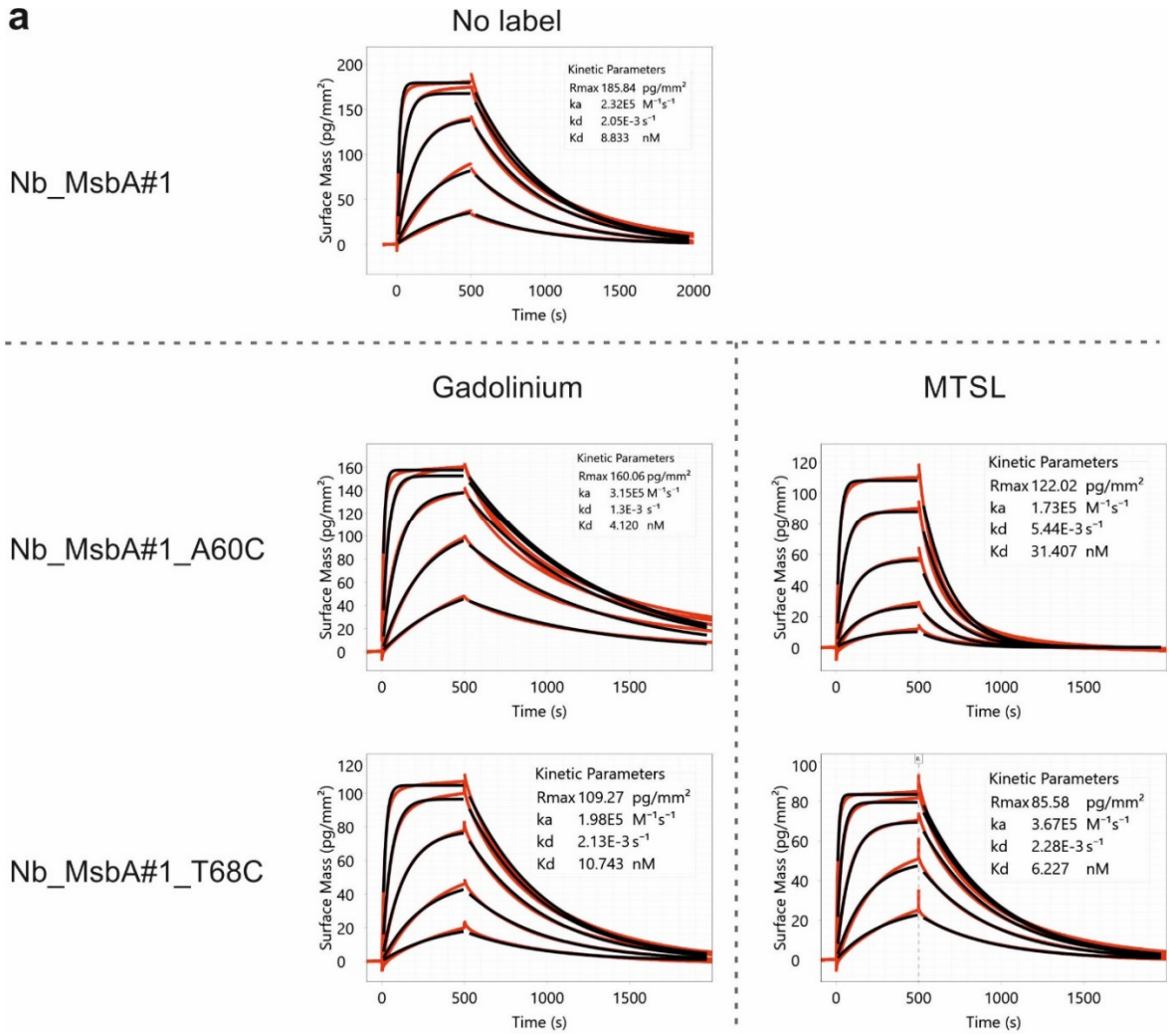
No label
Gadolinium
MTSL
Nb_MsbA#1
Nb_MsbA#1_A60C
Nb_MsbA#1_T68C
Kinetic Parameters
Rmax 185.84 pg/mm²
ka 2.32E5 M⁻¹s⁻¹
kd 2.05E-3 s⁻¹
Kd 8.833 nM
Kinetic Parameters
Rmax 160.06 pg/mm²
ka 3.15E5 M⁻¹s⁻¹
kd 1.3E-3 s⁻¹
Kd 4.120 nM
Kinetic Parameters
Rmax 122.02 pg/mm²
ka 1.73E5 M⁻¹s⁻¹
kd 5.44E-3 s⁻¹
Kd 31.407 nM
Kinetic Parameters
Rmax 109.27 pg/mm²
ka 1.98E5 M⁻¹s⁻¹
kd 2.13E-3 s⁻¹
Kd 10.743 nM
Kinetic Parameters
Rmax 85.58 pg/mm²
ka 3.67E5 M⁻¹s⁻¹
kd 2.28E-3 s⁻¹
Kd 6.227 nM
Surface Mass (pg/mm²)
Time (s)

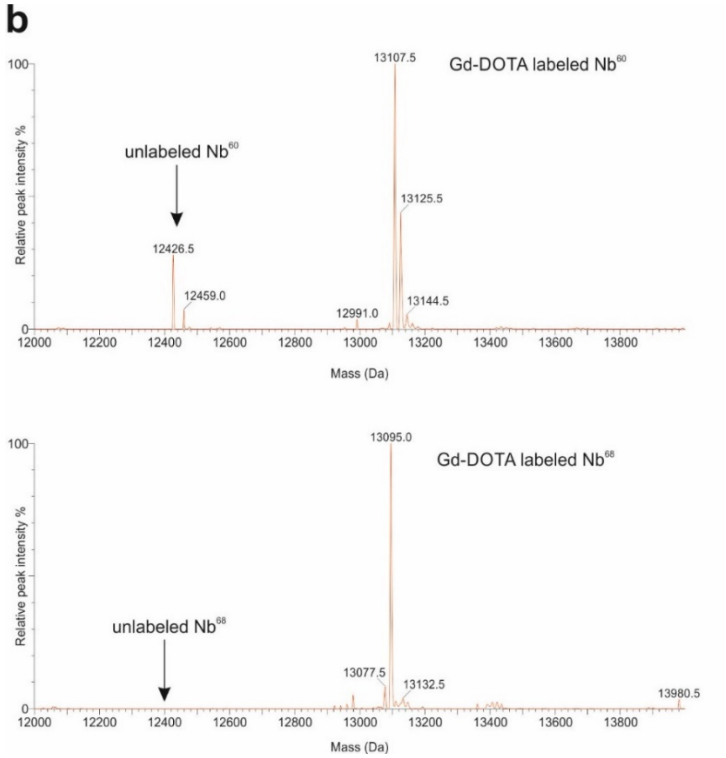


**Figure S2 | Affinity determination of Nb_MsbA#1 using grating coupled interferometry (GCI) and mass spectrometry analysis of Gd-labeled nanobodies. a,** GCI Measurements were conducted with biotinylated full-length MsbA immobilized on a WAVEchip and using unlabeled Nb_MsbA#1 as well as Nb_MsbA#1 labeled at amino acid positions 60 or 68 with Gd-DOTA or MTSL. Concentrations of injected nanobody were as follows: 3, 9, 27, 81 and 243 nM. Data were fitted to a 1:1 kinetic binding model and values for on-rates ($k_a$), off-rates ($k_d$) and dissociation constants ($K_D$) are directly given in the respective graphs. GCI measurements were carried out once. **b,** Mass spectrometry analysis of Nb_MsbA#1 labeled at position 60 or at position 68 with Gd-DOTA (expected mass shift upon labeling of 681 Da). The peaks of the labeled and unlabeled binders are marked. In case of the Gd-DOTA labeled nanobody at position 60, two peaks with a mass deviation of 18 Da are visible. The heavier mass peak corresponds to a water adduct. Based on the peak intensities, the labeling efficiencies were estimated as follows: Nb_MsbA#1_A60C: 80%, Nb_MsbA#1_T68C: 100%.

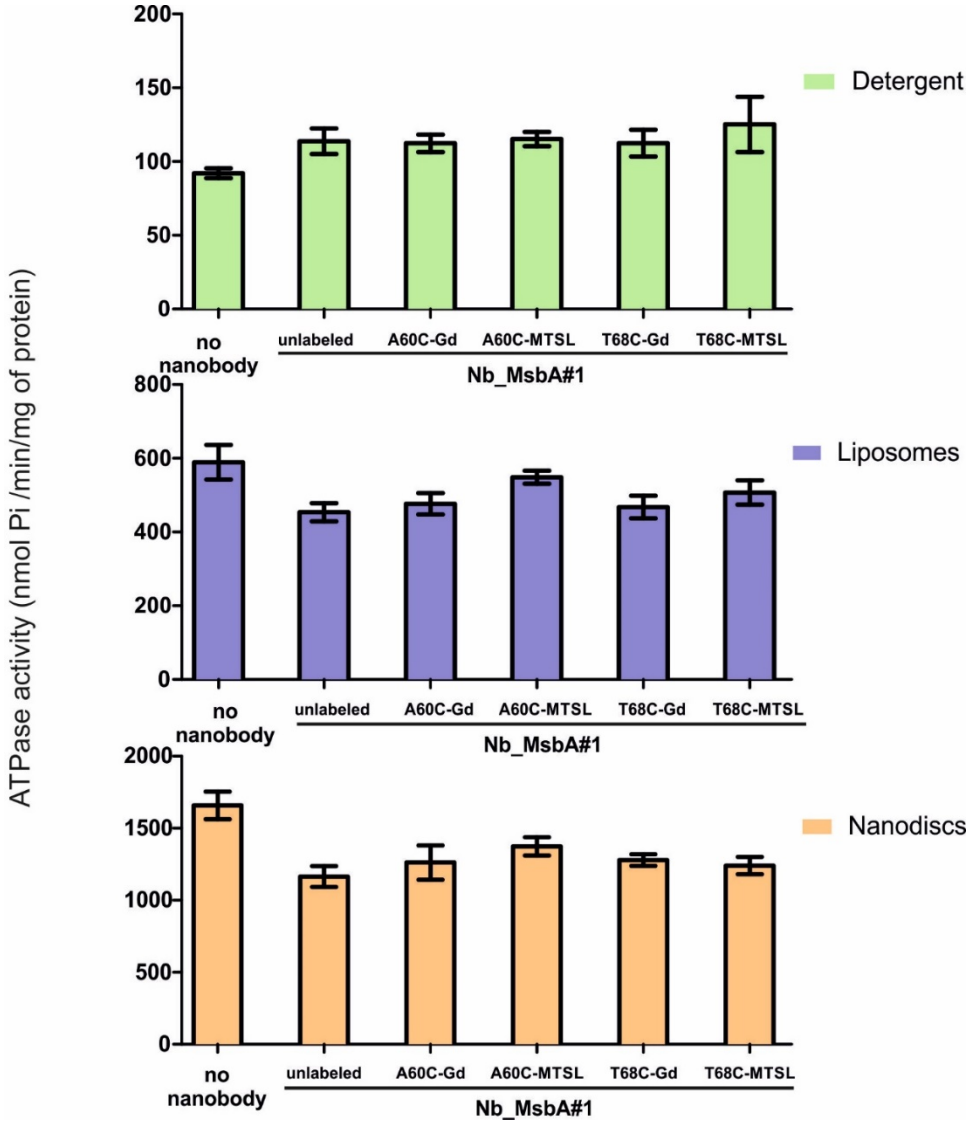


**Figure S3 | ATPase activity of MsbA in the presence of nanobody**. ATPase activity of MsbA in detergent, nanodiscs and liposomes was measured in the absence of nanobody (control), in the presence of 80 nM Nb_MsbA#1 (without label) or the corresponding Nb_MsbA#1 mutants labeled with Gd-DOTA or MTSL at positions 60 or 68. Error bars represent standard deviations of technical triplicates.

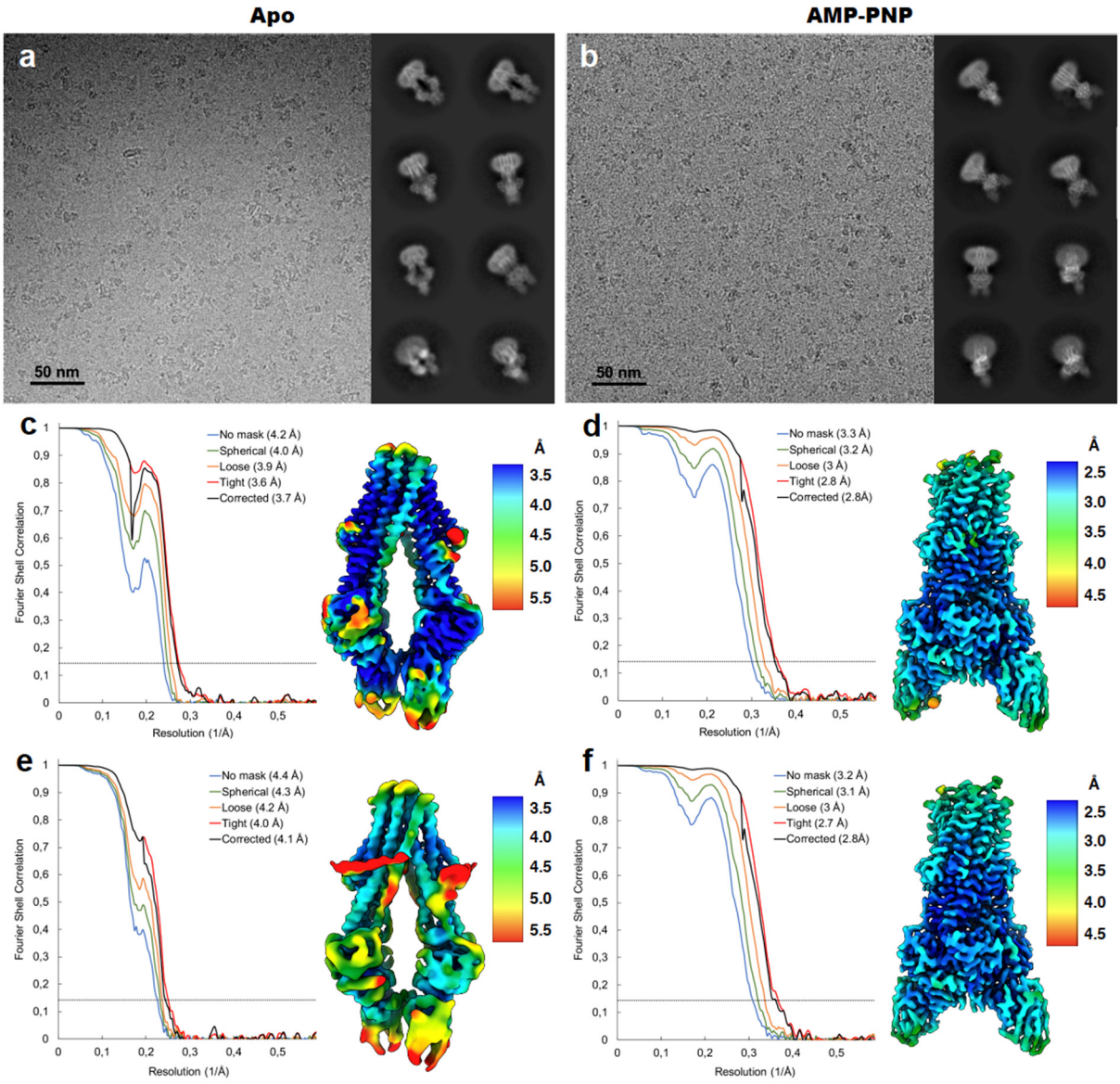


**Figure S4 | Cryo-EM analysis of nanodisc-reconstituted MsbA. a-b,** Typical micrograph and representative 2D class averages of MsbA-nanobody complex in absence of nucleotides **(a)** and in presence of AMPPNP-Mg **(b)**. **c-f**, FSC curves and local-resolution estimation for MsbA-60$^{Nb}$-IF$_{narrow}$ **(c)**, MsbA-60$^{Nb}$-OF$_{occluded}$ **(d)**, MsbA-68$^{Nb}$-IF$_{narrow}$ **(e)** and MsbA-68$^{Nb}$-OF$_{occluded}$ **(f)**.

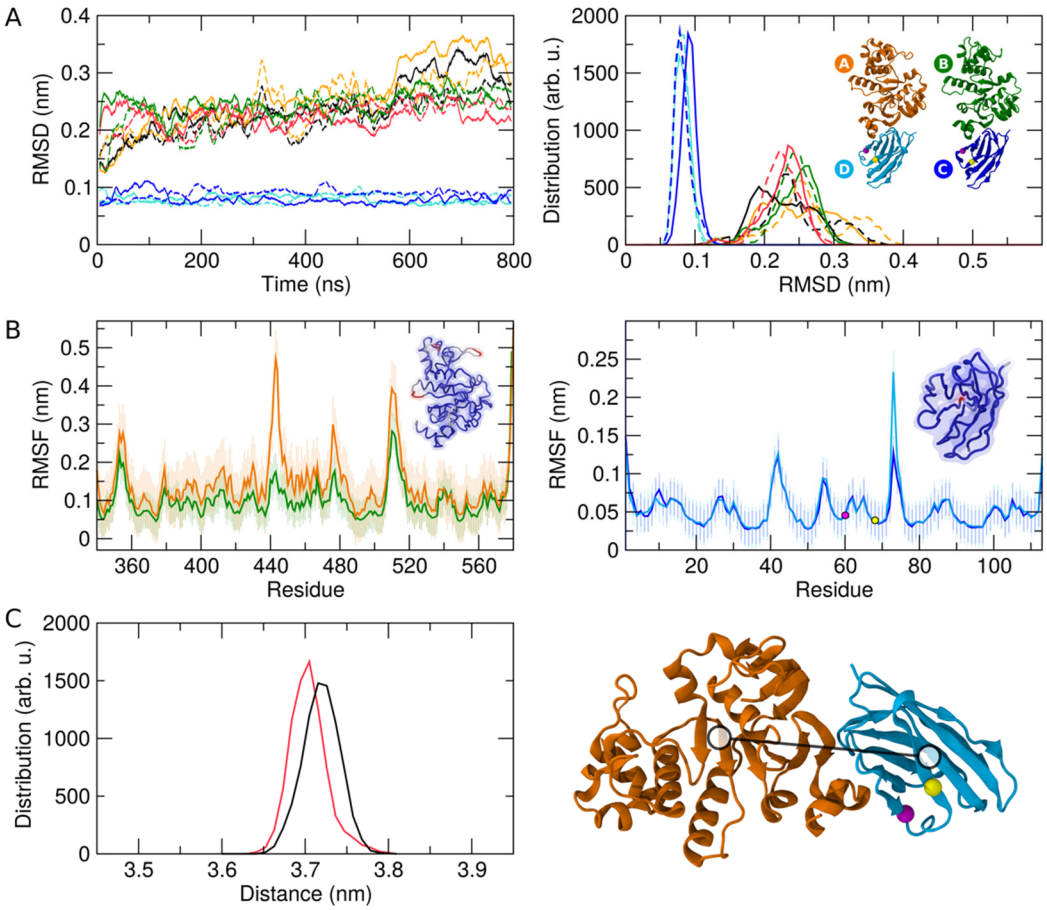


**Figure S5 | MD simulation based on the NBD-nanobody complex structure. a,** The root mean square deviation (RMSD) of Cα atoms from the starting structure of the simulations are plotted for NBD-Nb_1 (chains A and D; black curve) and NBD-Nb_2 (chains B and C; red curve). The first and second repeat simulations are indicated by dashed and straight lines, respectively. The RMSD values are also plotted for the individual NBDs (chains A and B) and nanobodies (chains C and D) with the color code indicated in the inset. In the RMSD time trace (left panel), the values have been averaged with a sliding window of length 5 ns. **b,** Root mean square fluctuations (RMSF) of Cα atoms are shown for the NBDs (left) and nanobodies (right). Colors are the same as in (a). The RMSF values have been averaged over the repeat simulations, the error is the standard deviation. The insets show the backbone structure colored from blue (low RMSF values) to red (high RMSF values). The positions of nanobody residues 60 and 68 are indicated. **c,** Distribution of the center of mass distance between NBD and nanobody (as schematically indicated at the right). The NBD-Nb_1 and the NBD-Nb_2 distances are shown in black and red, respectively.

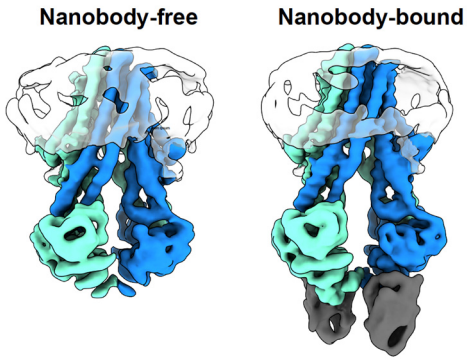


**Figure S6 | Impact of nanobody on the conformation of MsbA in nanodisc.** Cryo-EM reconstruction of nanobody free MsbA (at 4.9 Å resolution) compared to the reconstruction of nanobody-bound MsbA (at 4.2 Å resolution).

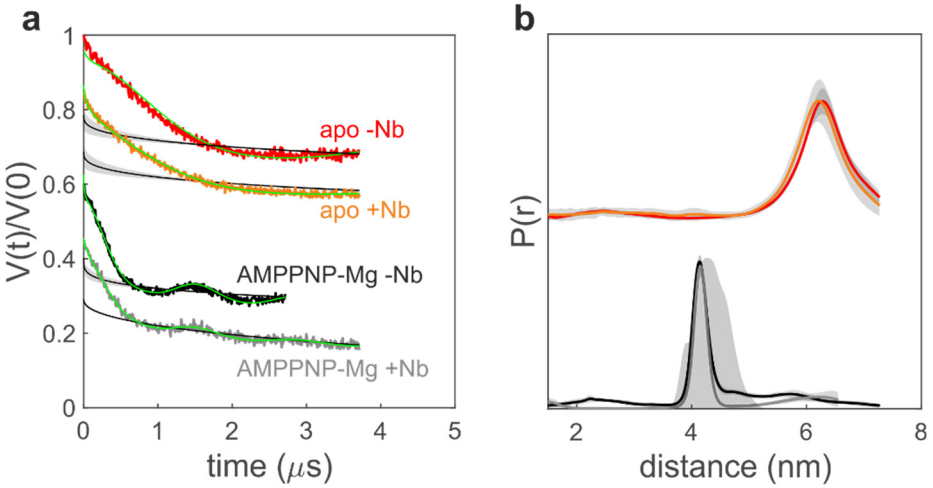


**Figure S7 | Impact of nanobody binding on MsbA's conformation in detergent. a,** Primary DEER data for detergent-purified MsbA labeled with MTSL at position 191 (intracellular region) in the absence (-Nb) and in the presence (+Nb) of the unlabeled Nb_MsbA#1 in the apo state (in red and orange) and in the AMPPNP-Mg state (in black and grey). Estimation of the background and fit of the primary data (in green) are also reported, together with the estimation of the relative uncertainties from DEERNet. **b,** Derived distance distributions for the four traces together with error estimation based on neural network analysis; the filled grey area for the AMPPNP-Mg state represents the rotamer-based prediction of the distance distribution for the outward-facing state (PDB used for the simulation: 3B5Y). Distance predictions for the apo state were not possible due to the lack of side chains in the low-resolution inward-facing crystal structure (PDB: 3B5W). Nanobody binding does not perturb the distance distributions of MsbA in any of the two states.

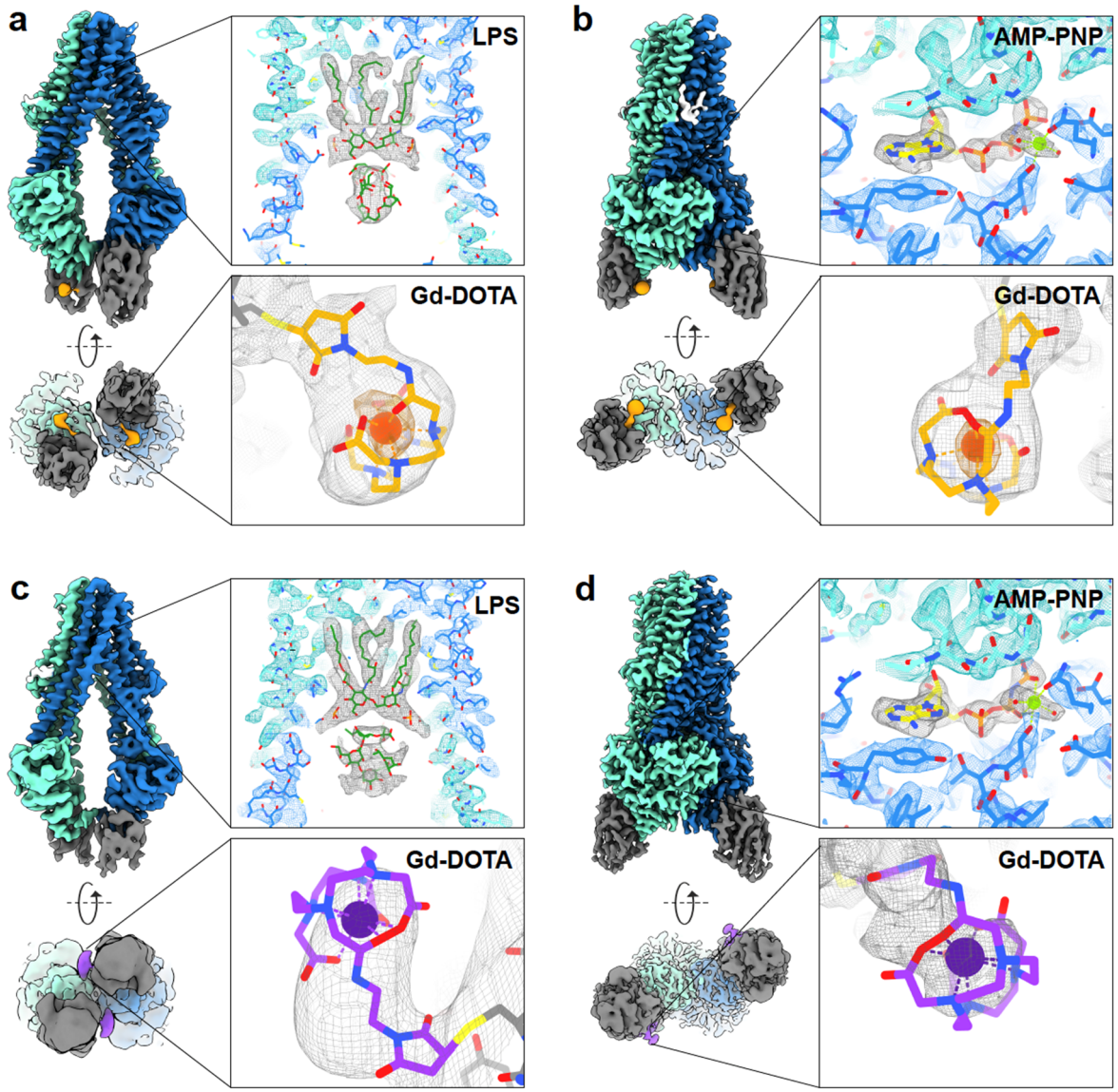


**Figure S8 | Cryo-EM maps and ligands. a,** The cryo-EM reconstruction of MsbA-60$^{Nb}$-IF$_{narrow}$ displays clear densities for LPS (green) and Nb$^{60}$ Gd-DOTA spin label (orange). **b**, Zoom-in on the nucleotide binding site and maleimide-Gd-DOTA label in the cryo-EM map of AMPPNP-Mg bound MsbA (MsbA-60$^{Nb}$-OF$_{occluded}$) demonstrates the quality of model to map fit. **c**, The cryo-EM map of MsbA-68$^{Nb}$-IF$_{narrow}$ is less resolved, especially at the lower part of the nanobodies, limiting the accuracy of Gd-DOTA modeling. The densities for 68$^{Nb}$ spin label (purple) are only visible at very low threshold. To enable their visualization, the bottom view of the map is displayed at a different threshold than the side view. **d,** The overall quality of MsbA-68$^{Nb}$-OF$_{occluded}$ reconstruction allows to unambiguously model AMPPNP-Mg together with two water molecules coordinating magnesium ion. However, the densities for Gd-DOTA (purple) are poor, indicating that the spin label at position 68$^{Nb}$ is not rigid. Similar as in (**c**), the bottom view is shown at a lower threshold to display week densities for Gd-DOTA. Color code as in main Fig. 1: MsbA – aquamarine/blue, LPS – green, Nb$^{60}$ Gd-DOTA – orange, Nb$^{68}$ Gd-DOTA (purple), lipid – white (only visible in **(b)**).

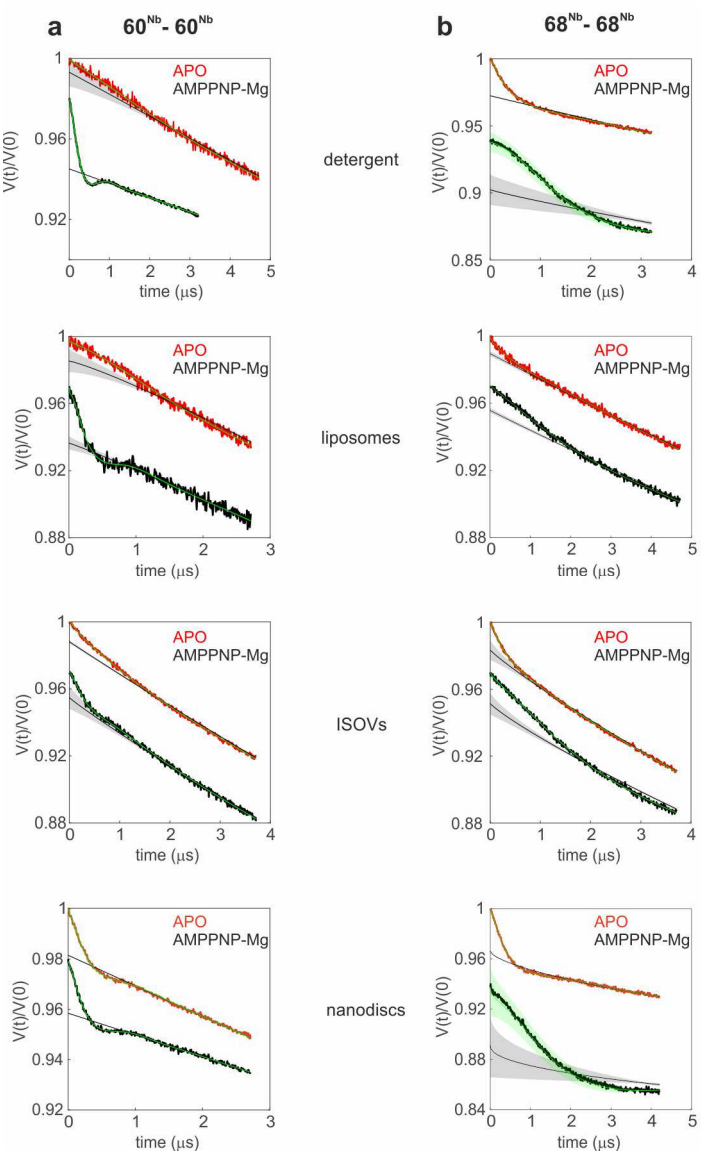


**Figure S9 | Primary DEER data related to main Fig. 2.** Primary DEER traces for the pairs $60^{Nb}$-$60^{Nb}$ (**a**) and $68^{Nb}$-$68^{Nb}$ (**b**) labeled with Gd-DOTA in the apo state (red traces) and in the AMPPNP-Mg state (black traces) for MsbA in detergent, reconstituted in nanodiscs or proteoliposomes and overexpressed in inside-out vesicles (ISOVs). The estimation of the background and fit of the primary data (in green) is reported, together with the estimation of the relative uncertainties by DEERNet.

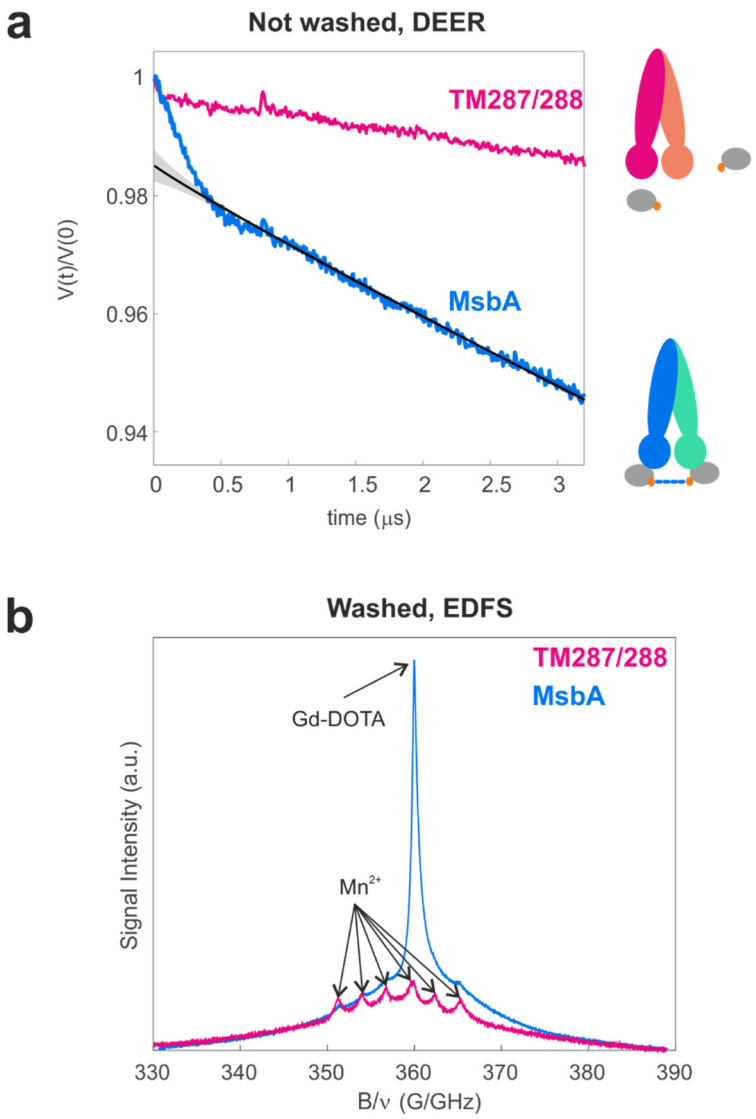


**Figure S10 | Specificity of nanobody binding to MsbA in *E. coli* ISOVs. a,** Primary DEER traces for the pair $60^{Nb}$-$60^{Nb}$ in ISOVs containing overexpressed TM287/288 (magenta) or overexpressed MsbA (light blue). The absence of a dipolar modulation in TM287/288-containing ISOVs demonstrates the high specificity of nanobody Nb_MsbA#1 towards MsbA, as sketched at the right panel. The ISOVs were not washed to remove unbound nanobodies prior to analysis. **b,** Echo-detected field sweep (EDFS) recorded at 10 K for ISOVs containing overexpressed TM287/288 (magenta) or MsbA (light blue). ISOVs were washed prior to this analysis to remove unbound nanobody. The Gd-maleimide-DOTA peak and the six hyperfine peaks of $Mn^{2+}$ ions originating from the broken cells are highlighted with black arrows. The gadolinium signal arising from the bound nanobodies is the most predominant feature in the spectrum for ISOVs containing overexpressed MsbA. For ISOVs containing TM287/288, the manganese signal is predominant due to a lack of Gd-labeled nanobody bound to their target protein. The x-axis of the spectra was frequency-normalized for better comparison.

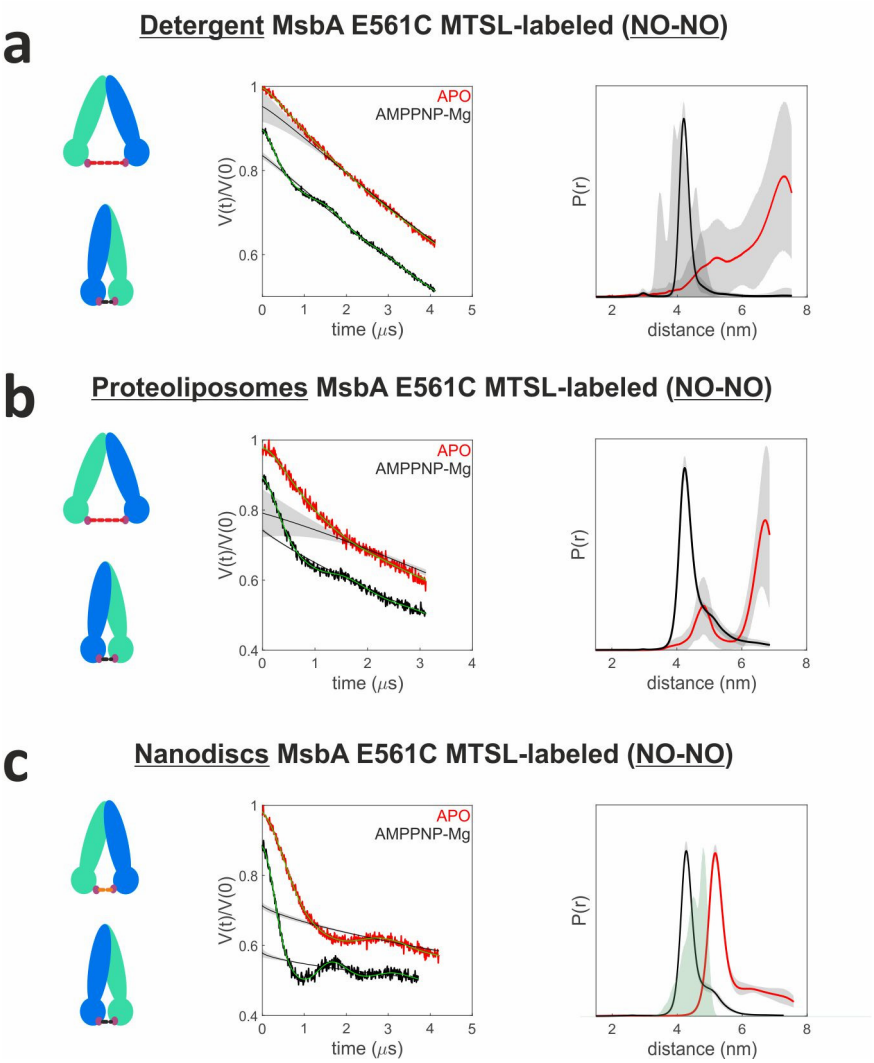


**Figure S11 | DEER analysis of nitroxide-labeled MsbA_E561C in different environments**. **a**-**c**, Primary nitroxide-nitroxide (NO-NO) DEER data (left) and corresponding distance distributions (right) for MTSL-labeled MsbA_E561C in detergent (**a**), proteoliposomes (**b**) and nanodiscs (**c**) in the apo and AMPPNP-Mg state in the absence of the nanobody. Where possible, distances were compared with simulations obtained on the crystal structure (grey filled area in panel a, X-ray structure of AMP-PNP MsbA in detergent (PDB: 3B5Y)) or the cryo-EM structure (green filled area in panel **c**, cryo-EM structure of apo MsbA in nanodiscs (PDB: 5TV4)). In agreement with the DEER analysis based on Gd-labeled nanobody as shown in main Fig. 2, also this analysis revealed shorter inter-NBD distances for apo MsbA_E561C in nanodiscs (**c**, red), compared to the corresponding traces in detergent (**a**, red) and proteoliposomes (**b**, red).

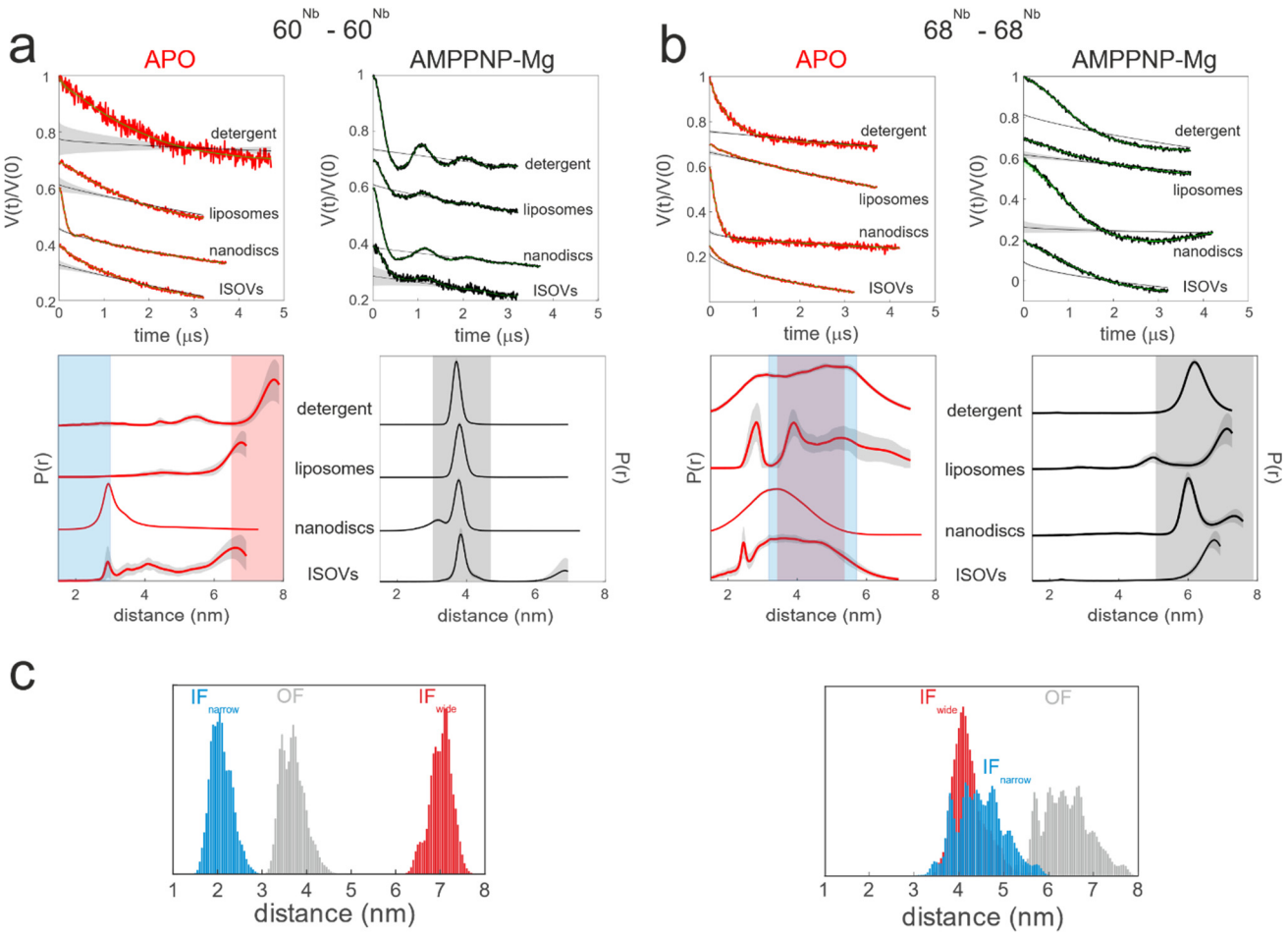


**Figure S12 | Nitroxide-labeled nanobodies probing MsbA in different environments**. Primary DEER traces for the pairs $60^{Nb}$-$60^{Nb}$ (**a**) and $68^{Nb}$-$68^{Nb}$ (**b**) labeled with MTSL in the apo state (red curves, left panels) and in the AMPPNP-Mg state (black curves, right panels) for MsbA in detergent, reconstituted in nanodiscs or proteoliposomes and MsbA overexpressed in inside-out vesicles (ISOVs). Lower modulation depths observed in the ISOVs data are due to the presence of residual reducing agents in the samples. Estimation of the background and fit of the primary data (in blue) are reported, together with the estimation of the relative uncertainties by DEERNet. Distance distributions are reported below the corresponding primary data. Uncertainties estimated from the neural network analysis are given for each distribution as a grey shaded band above and below the respective trace. The shaded areas represent the range of expected inter-nanobody distance distributions based on the MMM simulations shown in **c**, where the nanobody has been docked onto the following structures: $IF_{wide}$, X-ray structure of apo MsbA in detergent (PDB: 3B5W), in red; $IF_{narrow}$, cryo-EM structure of apo MsbA in nanodiscs (PDB: 5TV4), in blue; OF, X-ray structure of AMPPNP-Mg bound MsbA in detergent (PDB: 3B5Y), in grey.

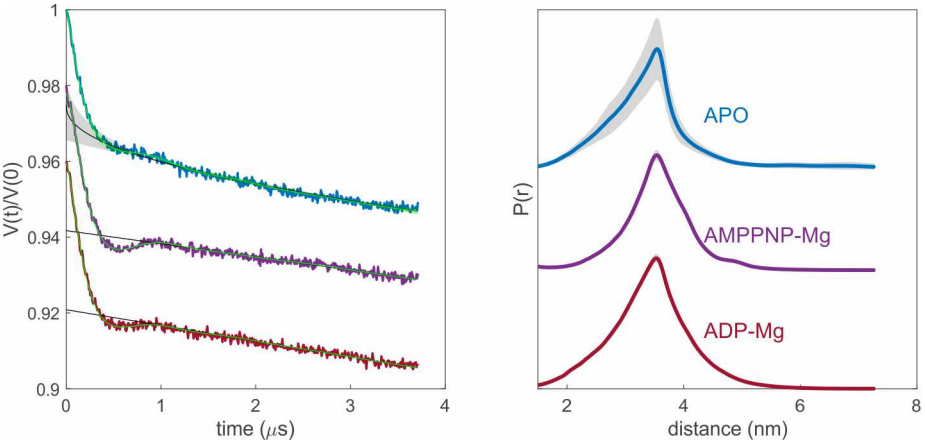


**Figure S13 | Invariant short $60^{Nb}$-$60^{Nb}$ distances in nanodiscs.** Primary DEER data (left) and corresponding distance distributions obtained with DEERNet (right) for the pair $60^{Nb}$-$60^{Nb}$ labeled with Gd-DOTA in nanodiscs in the apo state, after addition of AMPPNP-Mg and ADP-Mg (incubation of the sample with nucleotides at 37 degrees for 3 minutes).

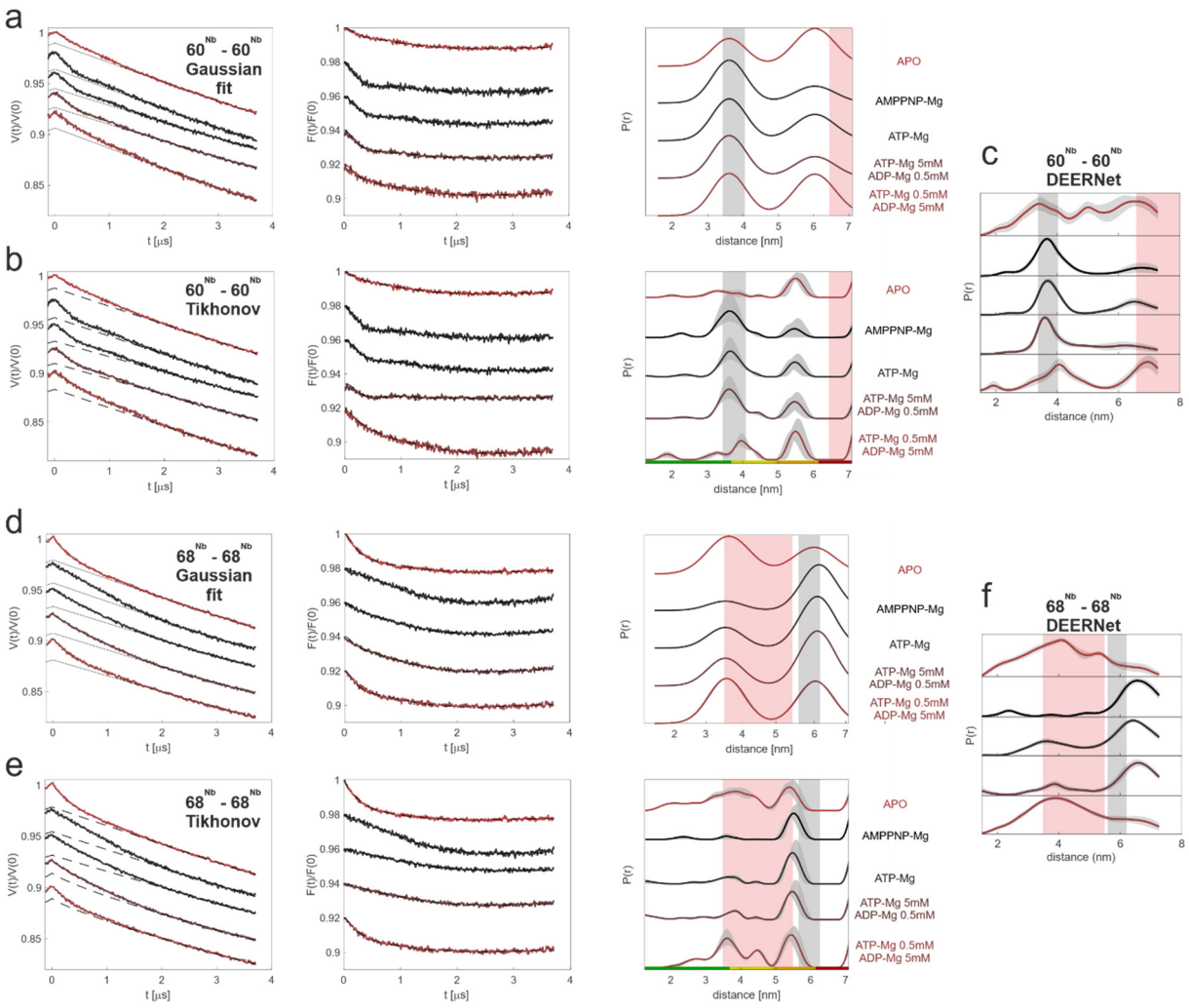


**Figure S14 | DEER data of Gd-labeled nanobodies probing MsbA in ISOVs under apo and ATP turnover conditions.**
Left: primary Gd-Gd DEER traces for the pair $60^{Nb}$-$60^{Nb}$ (**a** and **b**) and $68^{Nb}$-$68^{Nb}$ (**d** and **e**) in inside-out vesicles overexpressing wild-type MsbA, together with background fit (starting point of the background was 2000 ns for all traces). Middle: background-corrected DEER data and fit performed with Tikhonov regularization or model-based Gaussian fit. Right: corresponding distance distributions extracted using a Gaussian fit (**a** and **c**) (two Gaussians, mean distances and widths were fixed for each set of traces and only relative weights were fitted) and Tikhonov regularization (reg. parameter set to 1000, based on L-curve criterion, validation performed with background dimensions from 2.5 to 3.5, starting point for the background fit from 1500 to 2500, for a total of 30 trials) (**b** and **e**). A comparison with the results obtained using DEERNet (from main Fig. 3) is shown to highlight the robustness of the analysis (**c** and **f**). Shaded red and grey areas represent the expected distances for the $IF_{wide}$ and OF structures, respectively. All samples were incubated with an excess of Gd-labeled nanobody, washed and resuspended in deuterated buffer. ISOVs were incubated with respective nucleotides for 3 minutes at 37 °C prior to freezing.

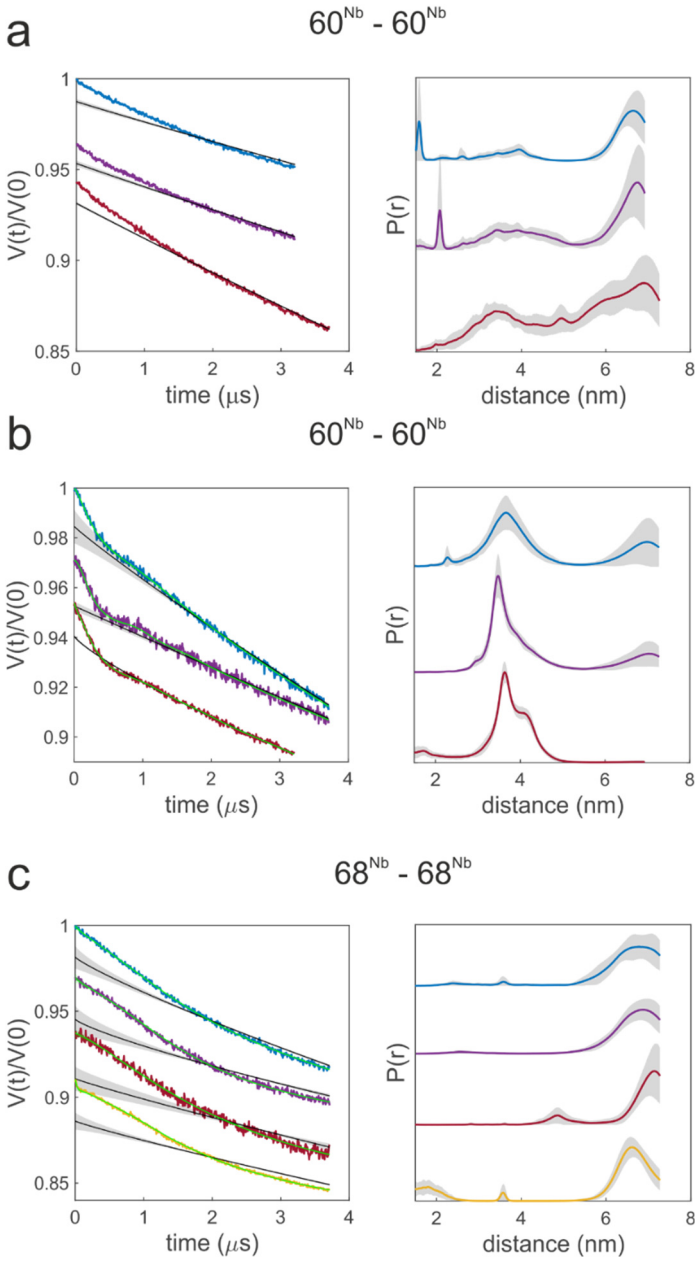


**Figure S15 | Biological repetitions of DEER data using ISOVs.** Primary DEER data (left) and corresponding distance distributions (right) obtained from different biological repetitions using ISOVs for the pairs $60^{Nb}$-$60^{Nb}$ in the apo state (**a**), in the AMPPNP-Mg state (**b**) and $68^{Nb}$-$68^{Nb}$ in the AMPPNP-Mg state (**c**). Samples were prepared starting from different batches of ISOVs and spin-labeled nanobodies. Each colored trace corresponds to a different biological repeat.

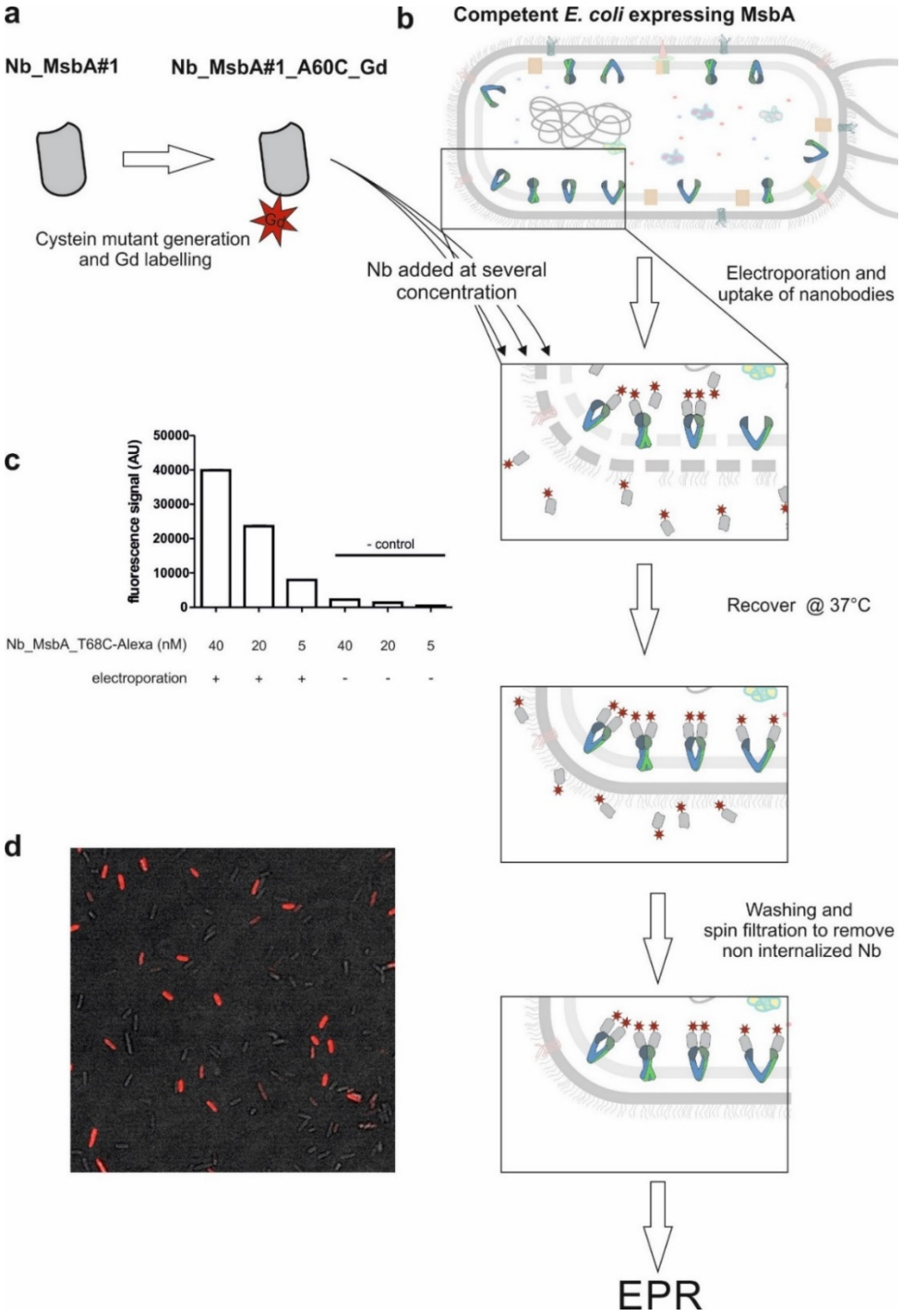


**Figure S16 | Sample preparation for in-cell DEER. a,** The nanobody is labeled with the Gd-DOTA maleimide spin label. **b,** Gd-labeled nanobodies (concentrations ranging from 20-30 µM) are electroporated into electrocompetent *E. coli* cells containing overexpressed MsbA. After recovery in culture media, non-internalized nanobody is removed by washing and spin filtration. Cells are finally frozen and analyzed by DEER. **c,** Result of a test experiment, in which fluorescently-labeled nanobody was electroporated. The bars show fluorescence intensities of electroporated *E. coli* after completion of entire workflow shown in (**b**). To assess background binding without internalization, samples without electroporation were used. **d,** Fluorescence microscopy analysis of *E. coli* cells electroporated with fluorescently-labeled nanobody.

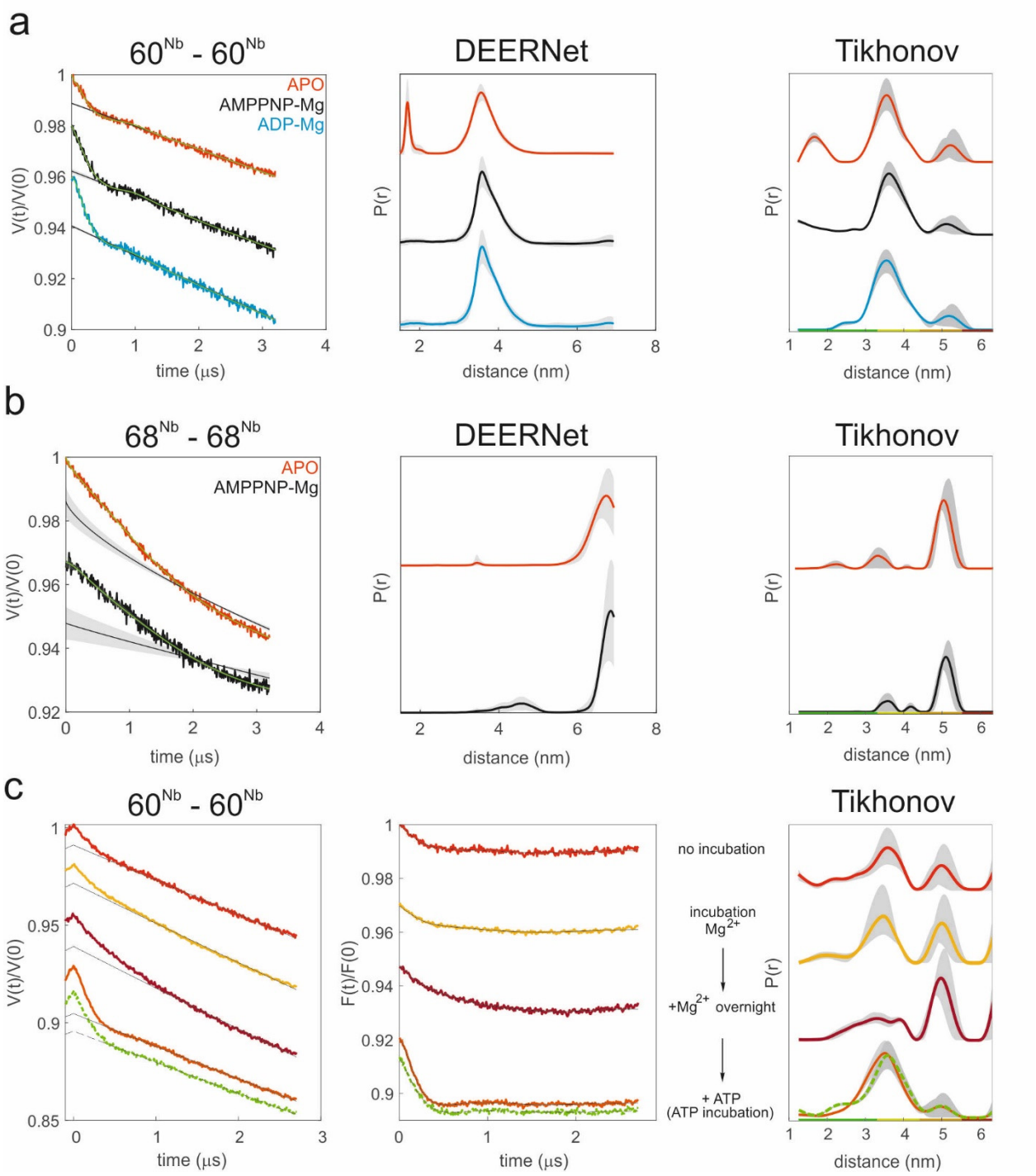


**Figure S17 | DEER analysis of *E. coli* ISOVs containing overexpressed MsbA_E506Q**. (**a** and **b**) Left: primary gadolinium-gadolinium DEER traces for the pair $60^{Nb}$-$60^{Nb}$ (**a**) and $68^{Nb}$-$68^{Nb}$ (**b**) in inside-out vesicles containing overexpressed MsbA_E506C in the apo (red), and AMPPNP-Mg state (black), together with background estimation and fit (in green). Middle: corresponding distance distributions obtained with DEERNet, together with uncertainty estimation. Right: distance distribution obtained with Tikhonov regularization (alpha parameter 1000, 3D background fit). The distance peak < 2 nm in the red distance distribution in panel **a** is due to an artifact present in the time trace close to the zero time. (**c**) Primary (left), background-corrected (middle) DEER data and corresponding distance distributions obtained via Tikhonov regularization (right) for ISOVs containing overexpressed MsbA_E506C in different experimental conditions to verify the residual bound ATP. The same sample of ISOVs was first measured with no addition of nucleotides (red, data comparable

to the biological repeat shown in the red trace in panel **a**). Afterwards it was thawed and incubated for one hour at 37 °C with 5 mM $MgCl_2$ to hydrolyze potential residual ATP (yellow), then thawed again and re-incubated at 37 °C with 5mM $MgCl_2$ overnight (purple). To verify the reversibility of the conformational transitions, the sample was once again thawed, and ATP was added (orange). The latter trace was compared to another sample from the same batch, which was immediately incubated with ATP, without freeze/thaw cycles (green). Data were analyzed using Tikhonov regularization (regularization parameter 1000, 3D background, 1000 ns background starting point) and validated (background dimensionality was varied from 2 to 3.5 and the background starting point from 800 to 1800 ns).

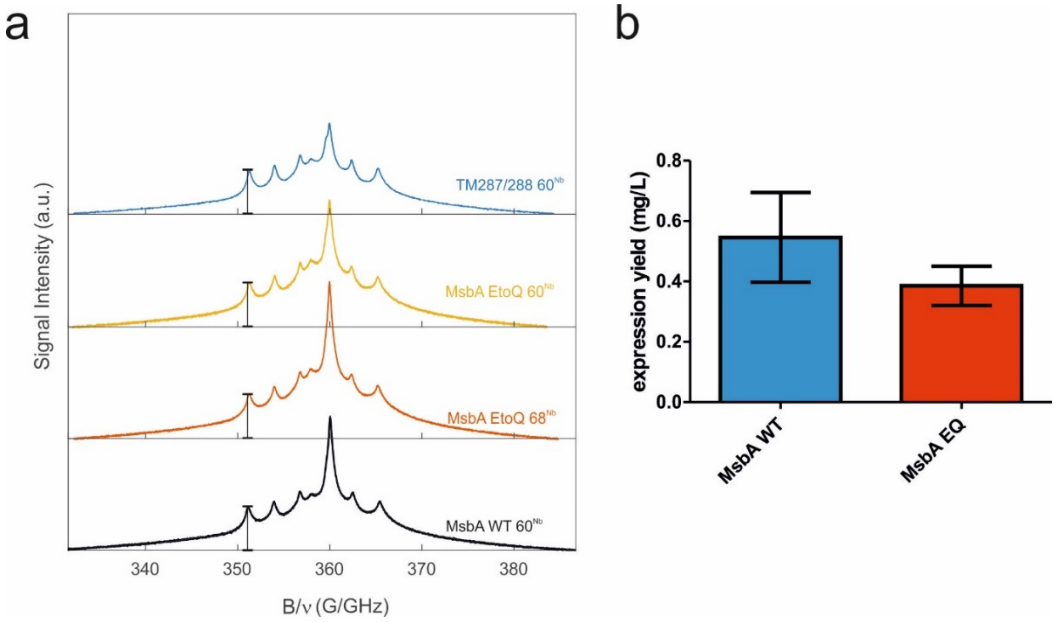


**Figure S18 | In-cell EDFS and expression levels of wild-type MsbA and MsbA_E506Q mutant in *E. coli*. a,** EDFS of *E. coli* cells overexpressing MsbA_E506Q or TM287/288 after electroporation and washing. Echo-detected field sweep measured at 10 K for *E. coli* cells overexpressing MsbA_E506Q after electroporation of 25µM of nanobody labeled with Gd-DOTA at position 60 or 68. As a control, cells overexpressing TM287/288 were electroporated with the nanobody labeled at position 60. The reported EDFS are those recorded on the samples shown in Fig. 4 in the main text. Note that the Gd-peak versus the manganese peaks is similarly strong for the MsbA and the TM287/288 sample, indicating that the Gd-labeled nanobody is equally present within the *E. coli* cell after electroporation and washing (as opposed to ISOVs, were the Gd-labeled nanobody is washed away and the Gd-signal is lost, see Fig. S11). **b,** MsbA WT and E506Q mutant were expressed and purified from *E. coli*. Protein yields (mg protein /expression culture volume) were calculated for three biological replicates.

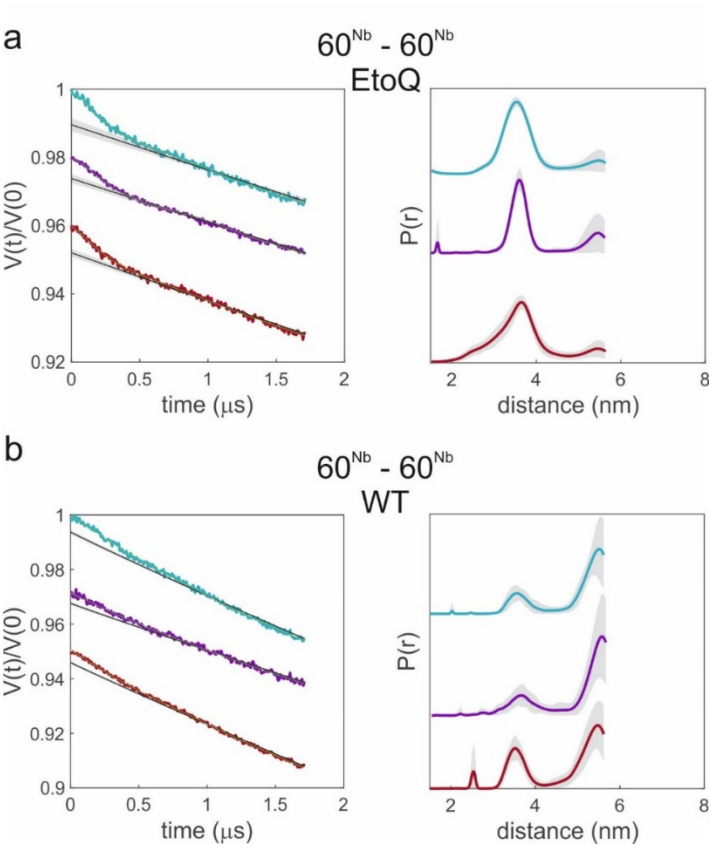


**Figure S19 | Biological repetitions of DEER data in *E. coli* cells.** Primary DEER data (left) and corresponding distance distributions (right) obtained from three biological repetitions (shown in blue, purple and red) for the pair $60^{Nb}$-$60^{Nb}$ in *E. coli* cells overexpressing MsbA_E506Q (**a**) or WT (**b**). All samples have been prepared starting from different batches of cells. The data of these three batches agree with the results of the fourth batch shown in Fig. 4. Nanobody concentrations in the electroporation buffer were 15, 20 and 25 µM (from top to bottom) for the MsbA_E506Q mutant and 20, 25 and 30 µM (from top to bottom) for MsbA WT, respectively. Lower nanobody concentrations were used for cells expressing the E506Q mutant to take into account the slightly different expression levels (see Fig. S18b).

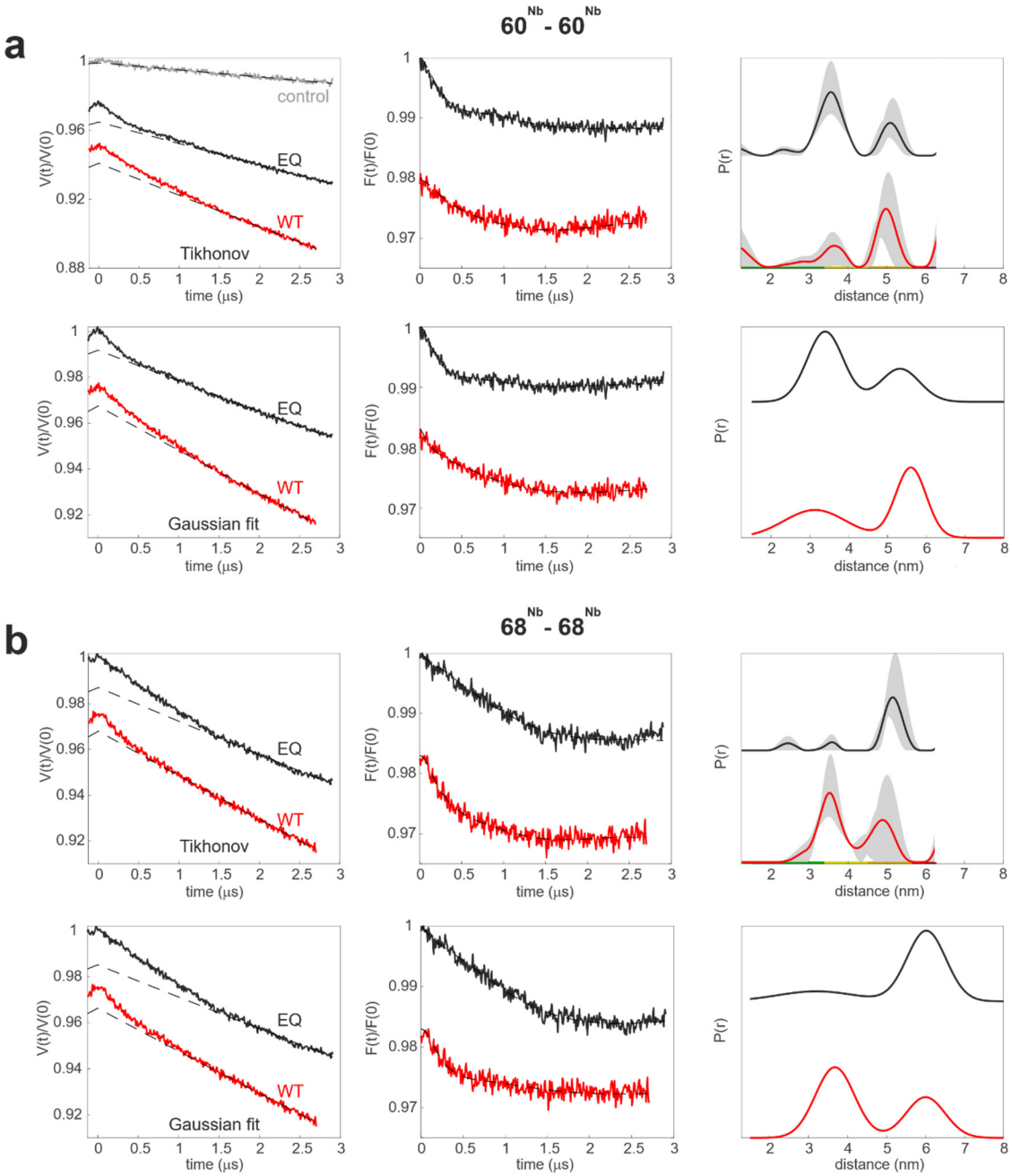


**Figure S20 | Comparative DEER analysis of MsbA in *E. coli* cells.** Primary DEER data (left), form factor (middle) and corresponding distance distributions (right) of the $60^{Nb}$-$60^{Nb}$ pair (**a**) and the $68^{Nb}$-$68^{Nb}$ pair (**b**) in cells overexpressing MsbA_E506Q (EQ, black) or wild-type MsbA (WT, red). A control sample (grey in **a**) with the Gd-labeled nanobody ($60^{Nb}$) electroporated in cells overexpressing TM287/288 did not show dipolar modulation. Data were analysed using Tikhonov regulation (top of both panels, reg. parameter 1000) and a model-based Gaussian fit (bottom of each panel, two Gaussian were used with main distance and width as free parameters). Tikhonov validation: background was varied from 700 to 1500 ns and background dimensionality from 2.5 to 3.5, for a total of 30 trials. All traces were analyzed and validated using the same parameters.

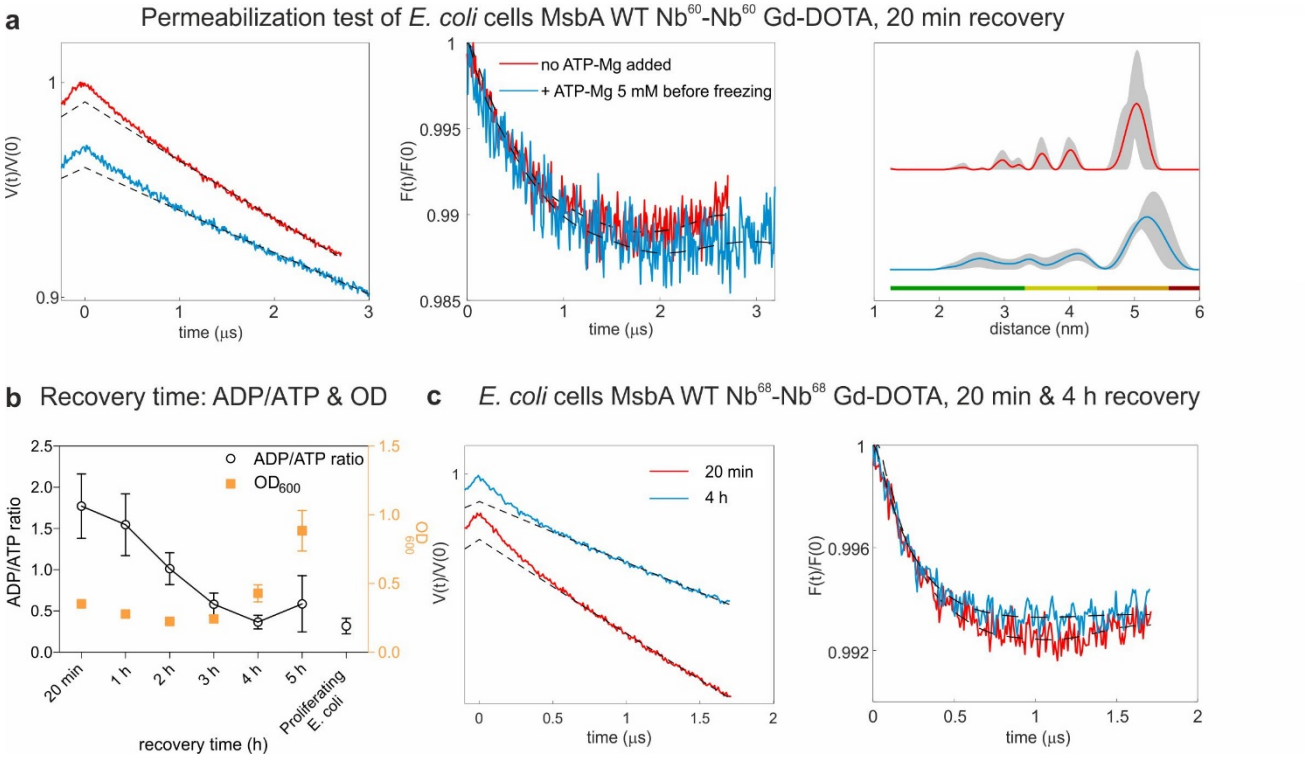


**Figure S21 | Control experiments on cell viability and integrity**. **a,** Cell permeability test. DEER traces recorded on the same *E. coli* cell batch overexpressing wild-type MsbA after electroporation with nanobodies labeled with Gd-DOTA at position 60 under normal experimental conditions (red) or upon addition of 5 mM ATP-Mg prior to freezing (blue). Left: Primary data. Center: background-corrected data. Right: distance distributions with validation. Data were analyzed as follows: Tikhonov regularization (reg. parameter set to 1000, based on L-curve criterion, validation performed with background dimensions from 2.5 to 3.5, starting point for the background fit from 600 to 2000, for a total of 30 trials. The short distance characteristic of the OF state did not become predominant after ATP addition, which indicates that electroporated cells are not permeable to ATP. **b,** ADP/ATP ratios and $OD_{600}$ of electroporated *E.coli* cells at different recovery times. The ADP/ATP ratio of proliferating *E. coli* cells is shown for comparison. After 4 h the ADP/ATP ratio is similar to that of proliferating *E. coli* cells, and $OD_{600}$ increases indicating full recovery. Error bars are standard deviations of technical triplicates. **c,** Primary (left) and background-corrected (right) DEER data of the same *E. coli* cell batch overexpressing wild-type MsbA after electroporation with nanobodies labeled with Gd-DOTA at position 68, recovered for 20 minutes (red) or 4 h (blue). Besides a different background, no notable differences were observed.

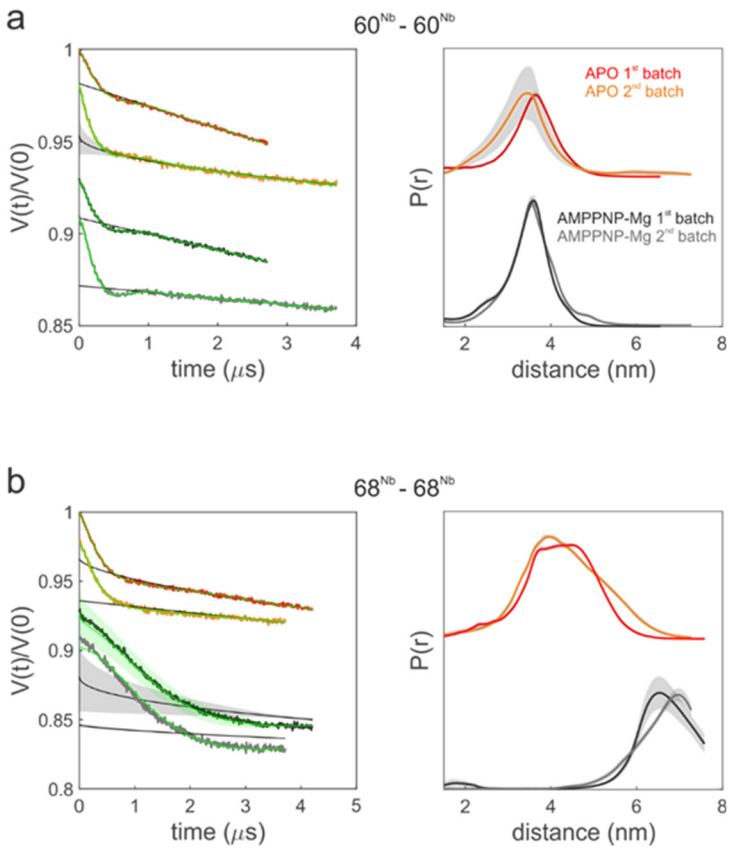


**Figure S22 | Biological repetition of DEER data in nanodiscs.** Left: primary gadolinium-gadolinium DEER traces for the pair $60^{Nb}$-$60^{Nb}$ (**a**) and $68^{Nb}$-$68^{Nb}$ (**b**) in two biologically independent preparations of nanodiscs (red and orange for first and second batch shown in the main Figs. 1 and 2) and AMPPNP-Mg state (black and grey for first and second batch shown in the main Figs. 1 and 2), together with background estimation and fit (in green). Right: corresponding distance distributions using DEERNet, together with error estimation.

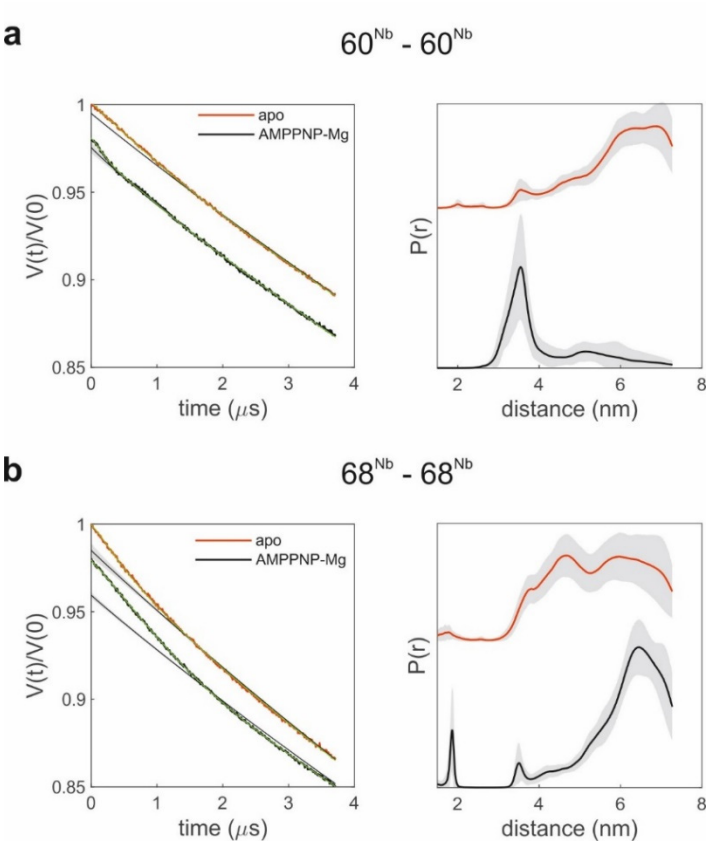


**Figure S23 | Biological repetition of DEER data in proteoliposomes.** Left: primary gadolinium-gadolinium DEER traces for the pair $60^{Nb}$-$60^{Nb}$ (**a**) and $68^{Nb}$-$68^{Nb}$ (**b**) in proteoliposomes in the apo (red) and AMPPNP-Mg state (black), together with background estimation and fit (in green). Right: corresponding distance distributions, together with error estimation. The data were collected from a biologically independent preparation of proteoliposomes compared to the one shown in main Fig. 2.

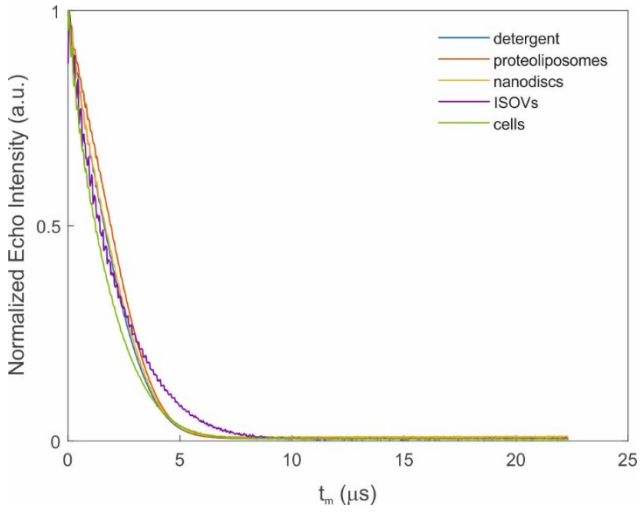


**Figure S24 | Hahn echo decays for the complex MsbA-nanobody labeled with Gd-DOTA in different environments.** Hahn echo decays have been measured at 10 K; sample compositions and sequence used are described in the Materials section.

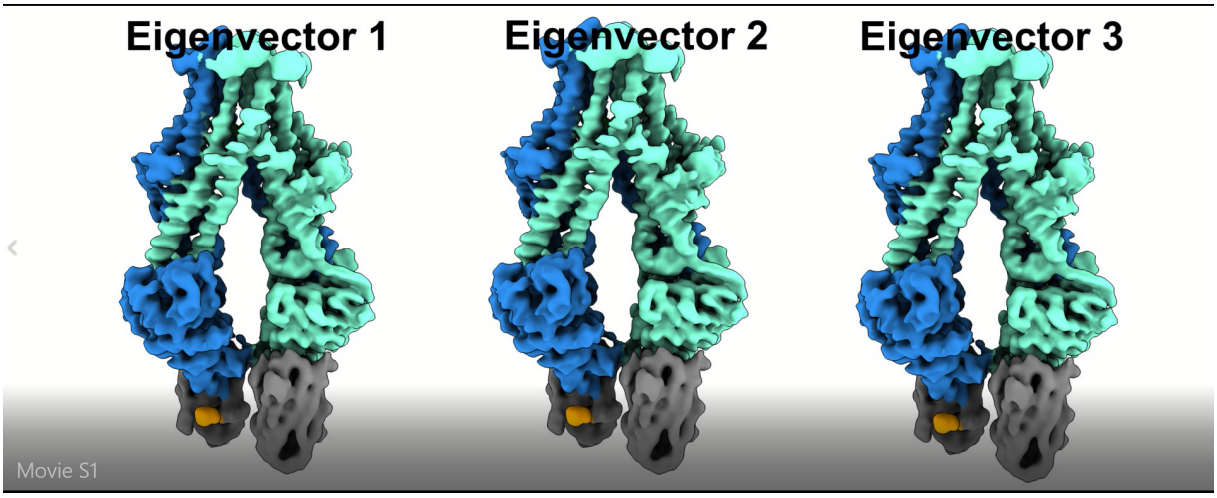


**Movie S1 | Analysis of MsbA-60$^{Nb}$-IF$_{narrow}$ using multi-body refinement.** Shown are movements along the three Eigenvectors.

**Table S1 | Crystallographic table of the NBD-nanobody complex**

Data collection and refinement statistics

| | |
|---|---|
| Data collection | |
| Space group | $P2_12_12_1$ |
| Cell dimensions | |
| *a*, *b*, *c* (Å) | 63.53 99.30 142.45 |
| α, β, γ (°) | 90.00 90.00 90.00 |
| Resolution (Å) | 2.1 (2.15 – 2.1) ‡ |
| $R_{merge}$ | 0.097 (1.332) |
| $I / \sigma I$ | 23.18 (2.29) |
| Completeness (%) | 100 (100) |
| Redundancy | 13.357 (12.388) |
| | |
| Refinement | |
| Resolution (Å) | 47.41 - 2.10 |
| No. reflections | 53383 (2613) |
| $R_{work}$ / $R_{free}$ | 0.2052/ 0.2439 |
| No. atoms | |
| Protein | 5447 |
| Water | 265 |
| *B*-factors | |
| Protein | 51.25 |
| Water | 47.41 |
| R.m.s. deviations | |
| Bond lengths (Å) | 0.005 |
| Bond angles (°) | 0.70 |

‡Values in parenthesis are shown for highest resolution shell.

**Table S2 | Cryo-EM data collection, refinement and validation statistics**

| | MsbA-nb60-Apo (EMDB-13404) (PDB 7PH2) | MsbA-nb60-AMPPNP (EMDB-13405) (PDB 7PH3) | MsbA-nb68-Apo (EMDB-13409) (PDB 7PH7) | MsbA-nb68-AMPPNP (EMDB-13406) (PDB 7PH4) |
|---|---|---|---|---|
| Data collection | | | | |
| Microscope | Titan Krios | Titan Krios | Titan Krios | Titan Krios |
| Camera | Gatan K3 Summit | Gatan K3 Summit | Gatan K3 Summit | Gatan K3 Summit |
| Voltage (kV) | 300 | 300 | 300 | 300 |
| Nominal magnification | 105,000 | 105,000 | 105,000 | 105,000 |
| Pixel size (Å) | 0.837 | 0.837 | 0.837 | 0.837 |
| Electron exposure (e–/Å$^2$) | 50 | 50 | 50 | 50 |
| Total exposure time (s) | 2.3 | 2.3 | 2.3 | 2.3 |
| Number of frames per image | 50 | 50 | 50 | 50 |
| Total number of images | 4662 | 4065 | 5502 | 8022 |
| Defocus range (μm) | -0.5 to -2.5 | -0.5 to -2.5 | -0.5 to -2.5 | -0.5 to -2.5 |
| Image processing | | | | |
| Processing software | RELION 3.1 | RELION 3.1 | RELION 3.1 | RELION 3.1 |
| Motion correction software | MotionCor2 | MotionCor2 | MotionCor2 | MotionCor2 |
| CTF estimation software | CtfFind4.1 | CtfFind4.1 | CtfFind4.1 | CtfFind4.1 |
| Particle selection software | RELION 3.1 | Topaz | Topaz | Topaz |
| Initial particle images (no.) | 1,761,489 | 535,889 | 1,651,657 | 2,078,720 |
| Final particle images (no.) | 142,832 | 109,465 | 247,610 | 132,288 |
| Final refinement software | CryoSPARC | CryoSPARC | CryoSPARC | CryoSPARC |
| Symmetry imposed | C2 | C2 | C2 | C2 |
| Map resolution (Å) | 3.7 | 2.8 | 4.1 | 2.8 |
| B-factor (Å$^2$) | -90 | -71 | -205 | -75 |
| Refinement statistics | | | | |
| Initial model (PDB code) | 5TV4, 7NDF | 5TTP, 7NDF | 5TV4, 7NDF | 5TTP, 7NDF |
| Modeling software | Coot, PHENIX | Coot, PHENIX | Coot, PHENIX | Coot, PHENIX |
| Model composition | | | | |
| Non-hydrogen atoms | 10699 | 10974 | 10695 | 10850 |
| Protein residues | 1362 | 1380 | 1362 | 1378 |
| Water molecules | - | 4 | - | 4 |
| Ligands | 18 | 12 | 18 | 10 |
| Mean *B* factors (Å$^2$) | | | | |
| Protein | 82.54 | 39.55 | 145.38 | 39.48 |
| Water molecules | - | 30.00 | - | 30.00 |
| Ligand | 123.82 | 55.79 | 192.65 | 59.29 |
| R.m.s. deviations | | | | |
| Bond lengths (Å) | 0.006 | 0.008 | 0.008 | 0.013 |
| Bond angles (°) | 0.871 | 0.849 | 1.006 | 1.120 |
| Validation | | | | |
| MolProbity score | 2.08 | 1.96 | 2.19 | 2.21 |
| Clashscore | 12.00 | 12.66 | 14.28 | 8.85 |
| Poor rotamers (%) | 0.09 | 0.26 | 0.09 | 0.6 |
| Ramachandran plot | | | | |
| Favored (%) | 91.88 | 94.97 | 90.77 | 95.47 |
| Allowed (%) | 7.98 | 4.96 | 9.16 | 4.45 |
| Disallowed (%) | 0.15 | 0.07 | 0.07 | 0.07 |

**Table S3 | MD simulations**

All-atom MD simulations

| System name | NBD atoms | Nanobody atoms | Water atoms | $Na^+$ ions | Total atoms | Box size (nm) |
|---|---|---|---|---|---|---|
| NBD-Nb_1[#] | 3764 | 1688 | 180180 | 5 | 185637 | $11.18^3$ |
| NBD-Nb_2[#] | 3744 | 1688 | 179804 | 5 | 185241 | $11.18^3$ |

Coarse-grained MD simulations

| System name | protein particles | Lipid particles | Water particles[&] | Ions ($Na^+$, $Cl^-$) | Total particles | Box size (nm) |
|---|---|---|---|---|---|---|
| $Msba\_IF_{wide}$ | 2488 | 8112 | 16381 | 558, 283 | 27822 | $3136^3$ |
| $Msba\_IF_{narrow}$ | 2488 | 8315 | 16315 | 565, 283 | 27966 | $3136^3$ |

[#]NBD-Nb_1 is composed of chains A and D, NBD-Nb_2 of chains C and B.
[&]A coarse-grained water particle represents 4 water molecules.